# Supplementary Materials: Towards Better Robustness against Common Corruptions for Unsupervised Domain Adaptation

Zhiqiang Gao*[1,2], Kaizhu Huang†[1], Rui Zhang[2], Dawei Liu[1], and Jieming Ma[2]

[1] Xi'an Jiatong-Liverpool University, Suzhou, China
{Zhiqiang.Gao, Rui.Zhang02, Jieming.Ma}@xjtlu.edu.cn
[2] Duke Kunshan University, Kunshan, China
{Zhiqiang.Gao, Kaizhu.Huang, Dawei.Liu}@dukekunshan.edu.cn

## 1. Dataset

**Office-31** [3] is a widely used dataset for evaluating visual domain adaptation algorithms. It comprises $4,652$ images and 31 categories from three distinct domains: Amazon (A), Webcam (W), and DSLR (D). We assess the performance of various methods using the following six transfer tasks: A→W, D→W, W→D, A→D, D→A, and W→A.

**Office-Home** [4] is a challenging dataset consisting of $15,500$ images across 65 classes from both office and home domains. This dataset spans four highly dissimilar domains: Artistic images (A), Clip Art (C), Product images (P), and Real-World images (R). Our evaluation encompasses all possible transfer tasks.

**VisDa-2017** [2] is a large-scale dataset tailored for visual domain adaptation tasks. It encompasses a total of $280K$ images distributed across 12 classes within training, validation, and test sets. In accordance with prior studies [1, 5], we utilize the training dataset, which comprises $152,397$ synthetic images, as the source domain. The validation dataset is comprised of $55,388$ real images and serves as the target domain. The performance assessment focuses on evaluating the effectiveness of a method in transferring knowledge learned from synthetic data to a real image dataset.

## 2. Sensitivity Analysis

Fig. 1(a) and (b) show the sensitivity analysis for the balancing parameters and adversarial data radius respectively. Three robust models are trained by deploying our DDAR method on UDA methods, i.e. MCC, MCC+CDAN, MCC+MDD, where the training and evaluation are conducted on the A→D task on the Office-31 dataset. In Fig. 1(a), the radius $\epsilon$ for generating adversarial data is set as 0.5. Then, we constrain the $\lambda_1 + \lambda_2 = 1$, where $\lambda_1$ and $\lambda_2$ are coefficients of supervised learning loss of source domain and adversarial regularization loss of target domain in Eq. 10 in the main paper. As such, the $(1.0, 0.0)$ represents training a standard model without using DDAR, which presents poor robustness against common corruption (RaCC). Once DDAR is involved in training, RaCCs are improved significantly, and the highest performances are obtained at $(0.6, 0.4)$. In Fig. 1(b), the $\lambda_1$ and $\lambda_2$ are set as 0.6 and 0.4 respectively. We evaluate the robust models trained by using adversarial data generated with different radius $\epsilon$. The $\epsilon = 0.0$ means no adversarial perturbations appear on data, where the model is trained by only using data augmented by VQGAN. As can be observed, the performance for RaCC increases with $\epsilon$, and the highest performances are attained when $\epsilon$ equals to 0.4 or 0.5.

*Majority of the work was done at Duke Kunshan University.
†Corresponding author.

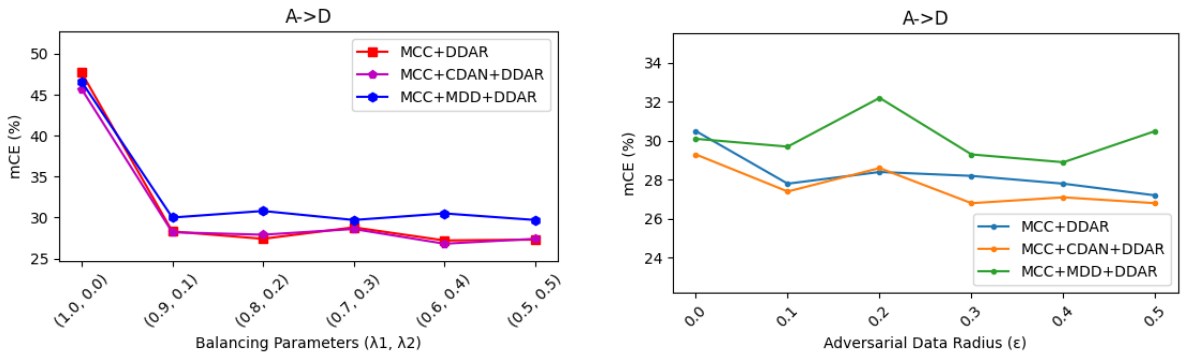


(a) (b)

Figure 1. Sensitivity analysis for the (a) balancing parameters and (b) adversarial data radius. All robust models are trained and evaluated on the A→D task on the Office-31 dataset.

## 3. Detail Results

The detailed results of Table 1-6 in the main paper are shown in Table 1-8 respectively.

| Method | A-D | A-W | D-A | D-W | W-A | W-D | Avg. (↓) |
|---|---|---|---|---|---|---|---|
| CDAN+TN | 60.3 | 59.6 | 64.1 | 83.5 | 64.7 | 120.2 | 75.4 |
| + Augmix | 46 | 65.2 | 66 | 59.9 | 67.9 | 64.3 | 61.6 |
| + DDG | 48.9 | 46.9 | 62.4 | 69.7 | 60.1 | 70.9 | 59.8 |
| DCAN | 42.3 | 40 | 50.3 | 45.2 | 60.1 | 46.6 | 47.4 |
| + Augmix | 40.5 | 32.4 | 53 | 48.1 | 59.8 | 54.6 | 48.1 |
| + DDG | 36.9 | 28.6 | 46.6 | 35.9 | 55 | 44.5 | 41.3 |
| MCC+DDAR | 27.2 | 28.5 | 49.9 | 21.2 | 53.7 | 23.1 | 33.9 |
| MCC+CDAN+DDAR | **26.8** | **26.3** | **44.8** | **19.0** | **46.7** | **19.4** | **30.5** |
| MCC+MDD+DDAR | 30.5 | 31.0 | 45.3 | 23.6 | 50.3 | 23.4 | 34.0 |

Table 1. Detailed results of Table 1 in main paper. **mCE** (↓) on Office-31 dataset under common corruptions (ResNet-50).

| Method | A-C | A-P | A-R | C-A | C-P | C-R | P-A | P-C | P-R | R-A | R-C | R-P | Avg. (↓) |
|---|---|---|---|---|---|---|---|---|---|---|---|---|---|
| CDAN+TN | 69.7 | 62.2 | 59.2 | 65.4 | 58.7 | 57.6 | 65.5 | 70.9 | 55.0 | 63.2 | 70.4 | 60.9 | 63.2 |
| + Augmix | 69.3 | 52.8 | 56.0 | 73.7 | 56.6 | 61.3 | 72.2 | 71.4 | 55.3 | 62.4 | 61.4 | 52.6 | 62.1 |
| + DDG | 59.8 | 52.2 | 48.0 | 66.0 | 51.9 | 56.2 | 63.6 | 63.6 | 48.8 | 57.8 | 64.4 | 47.9 | 56.7 |
| DCAN | 61.4 | 51.0 | 47.9 | 58.6 | 58.0 | 52.0 | 61.1 | 66.2 | 53.7 | 63.0 | 64.0 | 58.4 | 57.9 |
| + Augmix | 63.2 | 49.3 | 46.0 | 57.4 | 57.3 | 53.8 | 58.9 | 65.3 | 48.5 | 59.2 | 64.2 | 52.5 | 56.3 |
| + DDG | 58.3 | 48.0 | 44.6 | 55.2 | 51.6 | 47.5 | 55.1 | 62.2 | 49.4 | 57.7 | 59.9 | 52.6 | 53.5 |
| MCC+DDAR | 56.0 | 44.7 | **43.2** | 61.6 | 49.1 | 49.1 | 59.8 | 59.5 | 45.2 | 51.1 | 50.8 | **40.5** | 50.9 |
| MCC+CDAN+DDAR | **54.7** | **44.6** | 43.9 | **55.7** | **49.1** | **47.8** | **57.6** | **56.3** | 45.0 | 51.6 | **50.5** | 41.6 | **49.9** |
| MCC+MDD+DDAR | 69.5 | 48.7 | 46.3 | 68.2 | 50.7 | 49.8 | 58.5 | 67.2 | **44.7** | **49.6** | 53.3 | 42.6 | 54.1 |

Table 2. Detailed results of Table 1 in main paper. **mCE** (↓) on Office-Home dataset under common corruptions (ResNet-50).

| Method | Dataset | A-D | A-W | D-A | D-W | W-A | W-D | Avg. |
|---|---|---|---|---|---|---|---|---|
| MCC | Acc | 91.8 | 95.0 | 73.7 | 98.1 | 72.1 | 99.6 | 88.4 |
| | mCE | 47.7 | 46.1 | 57.8 | 36.6 | 60.2 | 34.9 | 47.2 |
| +DDAR | Acc | 93.0 | 89.7 | 71.0 | 98.5 | 69.2 | 99.8 | 86.8 |
| | mCE | 30.5 | 31.0 | 45.3 | 23.6 | 50.3 | 23.4 | 33.9 |
| MCC+CDAN | Acc | 94.0 | 94.8 | 75.5 | 98.4 | 75.0 | 100.0 | 89.6 |
| | mCE | 45.7 | 47.1 | 55.2 | 32.4 | 53.1 | 28.6 | 43.7 |
| +DDAR | Acc | 93.0 | 91.7 | 75.5 | 99.0 | 74.5 | 99.8 | 88.9 |
| | mCE | 26.8 | 26.3 | 44.8 | 19.0 | 46.7 | 19.4 | 30.5 |
| MCC+MDD | Acc | 93.8 | 94.2 | 74.6 | 98.6 | 74.7 | 99.8 | 89.3 |
| | mCE | 46.6 | 49.8 | 55.7 | 36.2 | 56.4 | 36.0 | 46.8 |
| +DDAR | Acc | 93.6 | 92.5 | 75.4 | 98.7 | 71.3 | 100.0 | 88.6 |
| | mCE | 30.5 | 31.0 | 45.3 | 23.6 | 50.3 | 23.4 | 34.0 |

Table 3. Detailed results of Table 2 in main paper. Standard accuracy (Acc) and **mCE** (↓) on Office-31 dataset under common corruptions (ResNet-50).

| Method | Dataset | A-C | A-P | A-R | C-A | C-P | C-R | P-A | P-C | P-R | R-A | R-C | R-P | Avg. |
|---|---|---|---|---|---|---|---|---|---|---|---|---|---|---|
| MCC | Acc | 57.2 | 77.7 | 83.3 | 64.9 | 76.6 | 78.2 | 65.1 | 54.3 | 82.5 | 73.3 | 61.8 | 86.7 | 71.8 |
| | mCE | 62.1 | 54.3 | 49.2 | 61.9 | 54.1 | 53.6 | 66.0 | 69.7 | 52.9 | 61.0 | 60.8 | 49.0 | 57.9 |
| +DDAR | Acc | 56.4 | 76.7 | 80.7 | 57.4 | 72.2 | 74.7 | 62.0 | 55.3 | 80.6 | 71.7 | 63.2 | 84.2 | 69.6 |
| | mCE | 56.0 | 44.7 | 43.2 | 61.6 | 49.1 | 49.1 | 59.8 | 59.5 | 45.2 | 51.1 | 50.8 | 40.5 | 50.9 |
| MCC+CDAN | Acc | 58.9 | 79.7 | 82.5 | 65.3 | 78.8 | 78.5 | 65.5 | 55.8 | 81.8 | 74.3 | 62.4 | 85.6 | 72.4 |
| | mCE | 60.5 | 51.8 | 49.4 | 61.6 | 51.5 | 49.4 | 63.2 | 65.0 | 51.3 | 58.9 | 58.7 | 47.9 | 55.8 |
| +DDAR | Acc | 58.1 | 77.5 | 80.3 | 65.1 | 73.9 | 76.0 | 65.2 | 58.5 | 81.1 | 72.8 | 64.1 | 84.2 | 71.4 |
| | mCE | 54.7 | 44.6 | 43.9 | 55.7 | 49.1 | 47.8 | 57.6 | 56.3 | 45.0 | 51.6 | 50.5 | 41.6 | 49.9 |
| MCC+MDD | Acc | 58.2 | 78.0 | 82.1 | 65.8 | 75.8 | 75.6 | 65.2 | 55.9 | 81.0 | 73.6 | 62.2 | 85.4 | 71.6 |
| | mCE | 62.2 | 54.5 | 53.1 | 63.0 | 58.9 | 57.1 | 65.5 | 69.5 | 55.3 | 62.3 | 61.8 | 51.6 | 59.6 |
| +DDAR | Acc | 43.3 | 74.7 | 79.6 | 51.4 | 72.5 | 73.2 | 63.6 | 48.8 | 81.7 | 73.8 | 62.7 | 83.6 | 67.4 |
| | mCE | 69.5 | 48.7 | 46.3 | 68.2 | 50.7 | 49.8 | 58.5 | 67.2 | 44.7 | 49.6 | 53.3 | 42.6 | 54.1 |

Table 4. Detailed results of Table 2 in main paper. Standard accuracy (Acc) and **mCE** (↓) on Office-Home dataset under common corruptions (ResNet-50).

| Method | A-D | A-W | D-A | D-W | W-A | W-D | Avg.(↓) |
|---|---|---|---|---|---|---|---|
| CDAN+MCC | 45.7 | 47.1 | 55.2 | 32.4 | 53.1 | 28.6 | 43.7 |
| CDAN+MCC+DDAR | 26.8 | 26.3 | 44.8 | 19.0 | 46.7 | 19.4 | 30.5 |
| w/o random start | 27.4 | 27.6 | 44.6 | 19.9 | 51.1 | 19.5 | 31.7 |
| w/o ID | 35.5 | 35.9 | 46.0 | 25.1 | 49.1 | 29.0 | 36.8 |
| w/o adversarial perturbation | 30.2 | 31.3 | 48.8 | 21.5 | 50.4 | 20.4 | 33.8 |

Table 5. Detailed results of Table 3 in main paper. **mCE** (↓) on corruptions of Office-31 dataset (ResNet-50)

| Method | A-D | A-W | D-A | D-W | W-A | W-D | Avg.(↓) |
|---|---|---|---|---|---|---|---|
| CDAN+MCC+Tent (epoch 10) | 16.6 | 27.7 | 86.1 | 19.7 | 84.9 | 6.2 | 40.2 |
| +DDAR | 10.1 | 19.6 | 69.9 | 11.6 | 82.3 | 3.0 | 32.7 |
| CDAN+MCC+Tent (epoch 1) | 16.3 | 23.4 | 63.1 | 13.6 | 61.2 | 5.2 | 30.5 |
| +DDAR | **9.6** | **14.3** | **59.1** | **6.1** | **61.2** | **1.9** | **25.4** |
| CDAN+MCC+AugMix+KL | 43.4 | 43.8 | 50.3 | 29.2 | 50.8 | 28.9 | 41.1 |
| CDAN+MCC+AugMix+W | 25.1 | 27.7 | **38.4** | 17.5 | **40.9** | 15.2 | 27.5 |
| +DDAR | **23.9** | **24.9** | 40.0 | **14.6** | 42.9 | **14.8** | **26.8** |
| CDAN+MCC+DeepAugment+KL | 41.3 | 40.0 | 45.2 | 29.6 | 45.0 | 29.2 | 38.4 |
| CDAN+MCC+DeepAugment+W | 22.9 | 22.9 | 39.8 | 14.9 | 40.3 | 15.1 | 26.0 |
| +DDAR | **19.4** | **20.8** | **36.9** | **12.8** | **37.0** | **12.5** | **23.2** |

Table 6. Detailed results of Table 4 in main paper. **mCE** (↓) on corruptions of Office-31 dataset (ResNet-50)

| Method | Adv. | Reg. | $\lambda_2$ | A-D | A-W | D-A | D-W | W-A | W-D | **Avg. (↓)** |
|---|---|---|---|---|---|---|---|---|---|---|
| VAT | KL | KL | 0.4 | 41.1 | 42.6 | 47.7 | 30.1 | 51.8 | 29.3 | 40.4 |
| TRADES-1 | KL | KL | 1 | 41.1 | 39.3 | 48.2 | 28.1 | 52.2 | 28.9 | 39.6 |
| TRADES-6 | KL | KL | 6 | 40.9 | 46.9 | 50.7 | 27.3 | 53.1 | 27.2 | 41.0 |
| AFD | CE | CDAN | 1 | 37.4 | 40.7 | 48.1 | 25.2 | 47.1 | 25.2 | 37.3 |
| D+KL | D | KL | 6 | 38.5 | 45.9 | 48.3 | 28.6 | 50.3 | 26.6 | 39.7 |
| D+CDAN | D | CDAN | 1 | 36.1 | 41.0 | 47.5 | 26.9 | 46.5 | 24.8 | 37.1 |
| CE+W | CE | W | 0.4 | 26.5 | 28.0 | 45.7 | 21.7 | 46.3 | 20.1 | 31.4 |
| KL+W | KL | W | 0.4 | **26.2** | 27.1 | 45.5 | 20.6 | 46.7 | 20.0 | 31.0 |
| DAAR | D | W | 0.4 | 26.8 | **26.3** | **44.8** | **19.0** | **46.7** | **19.4** | **30.5** |

Table 7. Detailed results of Table 5 in main paper. **mCE** (↓) on Office-31 dataset under common corruptions (ResNet-50).

| Method | Dataset | A-D | A-W | D-A | D-W | W-A | W-D | Avg. |
|---|---|---|---|---|---|---|---|---|
| Pixel-Space Perturbations | | | | | | | | |
| VAT | Acc | 91.4 | 93.5 | 74.0 | 98.5 | 72.1 | 99.6 | 88.2 |
| | mCE | 41.9 | 40.9 | 50.8 | 28.7 | 52.2 | 30.4 | 40.8 |
| AFD | Acc | 92.8 | 92.5 | 74.1 | 98.5 | 72.5 | 99.8 | 88.4 |
| | mCE | 40.0 | 41.8 | 47.2 | 28.4 | 49.1 | 27.8 | 39.0 |
| DDAR | Acc | 93.8 | 91.8 | 76.1 | 99.0 | 73.9 | 99.8 | 89.1 |
| | mCE | 35.5 | 35.9 | 46.0 | 25.1 | 49.1 | 29.0 | 36.8 |
| Image Discretization | | | | | | | | |
| VAT | Acc | 92.0 | 93.0 | 76.3 | 98.1 | 74.5 | 99.6 | 88.9 |
| | mCE | 41.1 | 42.6 | 47.7 | 30.1 | 51.8 | 29.3 | 40.4 |
| AFD | Acc | 89.8 | 89.7 | 75.3 | 97.5 | 73.3 | 99.4 | 87.5 |
| | mCE | 37.4 | 40.7 | 48.1 | 25.2 | 47.1 | 25.2 | 37.3 |
| DDAR | Acc | 93.0 | 91.7 | 75.5 | 99.0 | 74.5 | 99.8 | 88.9 |
| | mCE | 26.8 | 26.3 | 44.8 | 19.0 | 46.7 | 19.4 | 30.5 |

Table 8. Detailed results of Table 6 in main paper. Standard accuracy (Acc) and **mCE** (↓) for adversarial regularization methods based on pixel-space perturbations and image discretization on the Office-31 dataset (ResNet-50).

## References


[1] Mingsheng Long, Zhangjie Cao, Jianmin Wang, and Michael I Jordan. Conditional adversarial domain adaptation. In *Advances in neural information processing systems*, pages 1640–1650, 2018. 1

[2] Xingchao Peng, Ben Usman, Neela Kaushik, Judy Hoffman, Dequan Wang, and Kate Saenko. Visda: The visual domain adaptation challenge. *CoRR*, abs/1710.06924, 2017. 1

[3] Kate Saenko, Brian Kulis, Mario Fritz, and Trevor Darrell. Adapting visual category models to new domains. In Kostas Daniilidis, Petros Maragos, and Nikos Paragios, editors, *Computer Vision - ECCV 2010, 11th European Conference on Computer Vision, Heraklion, Crete, Greece, September 5-11, 2010, Proceedings, Part IV*, volume 6314 of *Lecture Notes in Computer Science*, pages 213–226. Springer, 2010. 1

[4] Hemanth Venkateswara, Jose Eusebio, Shayok Chakraborty, and Sethuraman Panchanathan. Deep hashing network for unsupervised domain adaptation. In *2017 IEEE Conference on Computer Vision and Pattern Recognition, CVPR 2017, Honolulu, HI, USA, July 21-26, 2017*, pages 5385–5394. IEEE Computer Society, 2017. 1

[5] Yuchen Zhang, Tianle Liu, Mingsheng Long, and Michael Jordan. Bridging theory and algorithm for domain adaptation. In *International Conference on Machine Learning*, pages 7404–7413, 2019. 1